Science Advances
AAAS
Manuscript Template

Hurricanes on Tidally Locked Terrestrial Planets

Jun Yang*, Mingyu Yan

Department of Atmospheric and Oceanic Sciences, School of Physics, Peking University, Beijing 100871, China.

*Corresponding author: junyang@pku.edu.cn

Abstract: Are there hurricanes on exoplanets? Tidally locked terrestrial planets around M dwarfs are the main targets of space missions for finding habitable exoplanets. Whether hurricanes can form on this kind of planet is important for their climate and habitability. Using a high-resolution global atmospheric circulation model, we show that hurricanes can form on the planets but not on all of them. For planets near the inner edge of the habitable zone of late M dwarfs, there are more and stronger hurricanes on both day and night sides. Hurricane theories on Earth are applicable when atmospheric compositions are similar to Earth. However, if background atmosphere is lighter than H_2O, hurricanes can hardly be produced because convection is always inhibited due to the effect of mean molecular weight, similar to that on Saturn. These results have broad implications on the precipitation, ocean mixing, climate, and atmospheric characterization of tidally locked planets.

Introduction

Hurricanes (also known as tropical cyclones or typhoons) are low-pressure weather systems with well-organized convection and are one of the most destructive disasters on Earth because they can induce strong winds, rapid increases in local sea level, and heavy precipitations (*1*,*2*). Hurricanes can also enhance the vertical mixing of heat and nutrients in the ocean, increase horizontal oceanic heat transport, and subsequently influence global climate (*3*-*5*). For instance, the curl of the strong winds can cause divergence and convergence in the upper ocean, producing regions of up-welling and down-welling and enhancing the exchanges between surface and subsurface oceans. Therefore, it is important and interesting to know whether hurricanes can form on other potentially habitable planets beyond Earth.

In this study, we focus on tidally locked terrestrial planets around M dwarfs, due to their relatively large planet-to-star ratios and frequent transits in observation. These planets differ from Earth in three major aspects: the uneven distribution of stellar energy between the permanent day and night sides, the slow rotation rate due to strong tidal force, and the redder stellar spectrum than the Sun. Several atmospheric general circulation models (AGCMs) have been employed and modified to simulate and understand atmospheric and climatic dynamics of the planets (*6*-*24*). These AGCMs have horizontal resolutions that are always equal to or larger than 300 km, so that most of their studies focus on planetary-scale phenomena, such as global-scale Walker circulation, equatorial superrotation, and forced Rossby and Kelvin waves. No work has investigated synoptic phenomena except Bin et al. (*25*). Based on the output data of an AGCM, they estimated genesis potential index of hurricanes and showed that the probability of hurricane formation is low for planets in the middle range of the habitable zone of M dwarfs. However, model resolution they used was not able to directly simulate hurricanes and whether the empirical index can be applied to exoplanets was unknown.

In this study, we explicitly simulate hurricane formation on tidally locked terrestrial planets with a high-resolution AGCM (see Materials and Methods). Horizontal resolution of the model is ≈50 km, under which the cyclogenesis, intensity, and structure of large hurricanes can be well resolved. The atmosphere is set to be dominated by N_2, O_2, CO_2, H_2, or He with a mean surface air pressure of 1 bar. Four different planetary rotation periods have been examined, 6, 10, 20, and 40 earth days. The surface is covered by seawater everywhere without land. Due to computation time limits, surface air temperatures are specified, but their magnitude and spatial pattern are set to be close to the results of relatively low-resolution AGCM simulations those have a slab ocean. We find that hurricanes can indeed form on the tidally locked planets but not on all of them.

Results

Hurricanes on tidally locked planets

Figure 1 shows the results of the control experiment for an aquaplanet orbiting close to the inner edge of the habitable zone around a late M dwarf of 2600 K. The rotation period is set to 6 earth days. Both the day and night sides are set to warm, and the day-to-night surface temperature contrast is small (see Fig. 2**A**). This experimental design is due to the fact that the day-to-night atmospheric latent heat transport is very efficient for planets near the inner edge (*9,10*). The high surface temperature, weak day-to-night contrast, and relatively fast rotation rate (comparing to planets in the middle range of the habitable zone or planets orbiting around hotter stars) benefit hurricane formation.

Clearly, there are hurricanes in the control experiment. In the mature stage of the hurricanes, maximum wind speed reaches ≈30-50 m s^{-1} (Fig. 1**A**), surface air pressure at the center is ≈950-980 hPa (Fig. 1**B**), precipitation reaches as high as 200-500 mm per day due to strong convection especially near the eyewall (Fig. 1**C**), and relative vorticity near the surface is in the order of 10^{-4} s^{-1} (Fig. 1**D**), close to those on Earth (*1,2*). The surface wind speed increases as the eyewall is

approached from outside, but inside the eyewall the winds as well as precipitation weaken rapidly. The winds rotate counter-clockwise in the northern hemisphere and clockwise in the southern hemisphere due to the Coriolis force although in this experiment it is much smaller than that on Earth. The precipitation exhibits well-defined spiral bands rather than uniformly distributed throughout the region of the hurricane. The clear patterns of eye–eyewall and spiral rain bands suggest that the model resolution of 50 km is good in resolving the hurricanes.

For vertical cross structure (Fig. S1), the tangential wind component dominates the flow through the system although the radial wind is also significant. In the boundary layer, the winds flow toward the low-pressure center. Within the hurricane, upward motion is robust and tilts radially outward. The maximum ascendance near the surface locates at a distance of ≈250 km outward from the hurricane center rather than at the center itself. Indeed, weak downward motion comprises the center. Due to the ascendance and deep convection, relative humidity is high in the hurricane. Latent heat release from the convection and adiabatic warming by compression from the subsidence in the eye produce a warmer region of air with temperatures of ≈4 K above the environmental value. This can be called as a "warm core", which is one of the most characteristic features of hurricane. The warm core can also be viewed from the equivalent potential temperature anomaly. Hurricanes on the night side (Fig. S2) are smaller in horizontal size compared to that on the day side, ≈500 versus 1500 km, but the vertical structures are similar.

Statistical analysis shows that in the control experiment there are four preferred regions for hurricane genesis: the northern and southern tropics of the day side near the substellar point and the middle-to-high latitudes of the night side on each hemisphere (black dots in Fig. 2**A**). Hurricane formation is largely determined by small-scale convection, large-scale environmental condition, and the interactions between them. Below, we explore the underlying mechanisms through two ways.

One way is the positive feedback between cumulus convection and larger-scale disturbance, known as the Conditional Instability of the Second Kind (CISK (*26-29*)). On tidally locked planets, long-term mean atmospheric circulation is characterized by large-scale Rossby waves on the west and pole of the substellar point and Kelvin waves on the east of the substellar point (Fig. 2**B**), excited from the uneven stellar radiation distribution (*6,31*). The wave pattern is similar to the tropical Matsuno-Gill pattern on Earth (*30,32*), but the meridional (south-north) scale is larger, ≈10,000 versus 3,000 km. The Rossby waves have one low-pressure center on each hemisphere, whose corresponding environmental vertical motion is updrafts and relative vorticity is positive (negative) on the northern (southern) hemisphere. This low pressure system favors the onset of the CISK feedback: Surface winds spiral into the low-pressure center and create horizontal convergence; this low-level convergence enhances relative vorticity through vortex stretching, increases upward motion following the conservation of mass, and meanwhile brings water vapor into the center, amplifying cumulus convection and release of latent heat; the latent heat release warms the air and lowers the air density through forcing more upper-level air to move outward away from the center, subsequently reducing the surface pressure; the lower surface pressure further enhances the low-level convergence and increases the growth rate of the relative vorticity through vortex stretching (Fig. 2**D-F**). This feedback is the key in promoting the growth of small-scale disturbances to hurricanes in the background low-pressure regions. It is similar to that on Earth: hurricane generally forms in the monsoon troughs and the confluence zones where the surface pressure is relatively low, collocated with high cyclonic vorticity, convergent surface winds, and divergent winds aloft (*1,2*). Moreover, during the formation phase, the latent heat flux from the surface to the boundary layer increases strongly (Fig. 2**G**), which also contributes to intensify the hurricane through the feedback of wind-induced surface energy exchange (WISHE (*2,28*)).

The lifetime of the hurricanes on the day side is ≈40-50 earth days, longer than that on Earth. This is mainly due to the absence of continents and the warm surface everywhere in the experiment. On the night side, the lifetime is shorter, ≈10-20 earth days.

Another way is the empirical equation of genesis potential index (GPI (*25*,*33*,*34*)). The index combines five environmental factors to predict the potential of hurricane formation, including planetary vorticity, relative vorticity, relative humidity, potential intensity, and wind shear (see Methods). Comparison between Figs. 2**A** and 3**A** reveals a positive correlation between the location of hurricane genesis and large values of GPI. In the four hurricane regions, GPI values are large because the relative vorticity is great, relative humidity is high, potential intensity is large, and/or vertical wind shear is weak (Fig. 3**B-F**). These favor hurricane formations there. For example, when the shear is strong, an initial disturbance will be ventilated by cooler or drier air and thereby temperature and moisture anomalies are hard to maintain (*35*). In this experiment, the vertical wind shear is strong especially in the tropics of the night side associated with atmospheric superrotation (*6*,*7*) and in the extratropics of the day side (Fig. 3**F**), so that there is nearly no hurricane formation there. Note that the applicability of the empirical GPI index on Earth to the tidally locked planet is mainly due to that we employed an earth-like atmosphere here; when the atmospheric composition is quite different from Earth, GPI is not a good index as addressed below.

The formation of hurricanes on the night side is surprising because the night side has no stellar radiation and the long-term mean vertical motion is downwelling rather than upwelling. In this experiment of planet close to the inner edge of the habitable zone, however, the night-side surface is warm, the surface temperature gradient is small (Fig. 2**A**), there are a few short-time small low-pressure regions (Fig. 2**C**), the planetary vorticity is relatively high (Fig. 3**B**), and the vertical wind shear is weak (Fig. 3**F**), at the middle-to-high latitudes. These factors promote hurricane genesis there. But, when the surface temperature is decreased or the rotation rate is slowed down, there is fewer or no hurricane on the night side (see below).

Effects of planetary rotation rate and surface temperature

In order to test the effect of rotation rate, we performed three experiments in which rotation period is increased (i.e., the rotation rate is decreased) while other experimental designs are left to be the same as that in the control experiment. In the case of 10 days, the hurricane frequency does not change much on the day side but decreases significantly on the night side (Fig. 4**A**). In the case of 20 days, there is nearly no hurricane on the night side and the number of hurricanes on the day side also decreases largely (Fig. 4**B**). For the case of 40 days, hurricane only forms at regions very close to the substellar point (Fig. 4**C**). This trend as a function of rotation period is mainly due to three factors: the direct weakness of planetary vorticity, the reduction of relative vorticity due to that the atmosphere becomes so steady that waves and disturbances become less active, and the decrease of relative humidity on the night side (but increase on the day side) due to the strengthening of the thermal-driven global Walker circulation (Fig. S5).

When the surface temperature is decreased, hurricane is also harder to form. As the maximum surface temperature is set to 308 K and the night-side surface temperature is set to 275 K, fewer hurricanes form in the vicinity of the substellar point and no hurricane on the night side (Fig. 4**D**). When the maximum surface temperature is set to 301 K and the night-side surface temperature is set to 268 K, there are only two hurricane events during the integration of four earth years (Fig. 4**E**), consistent with the GPI prediction in Bin et al. (*25*). Note that the temperature of 301 K is close to the tropical surface temperatures on Earth. This suggests hurricane formation on tidally locked planets requires a warmer surface, due to their slower rotation rates and stronger wind shears. For planets with both slow rotation and low temperature, no hurricane can form (Fig. 4**F**). The decreasing trend of hurricane formation as a function of reduced surface temperature is due to two main processes: the relative humidity and potential intensity decrease because of the cooler surface and weaker upwelling and convection, and the vertical wind shear becomes much stronger due to the enhanced temperature gradients between day and night sides (Fig. S6). Moreover, when the

night-side surface temperature is low, air convergence from the night side to the day side brings cool air rather than warm air into the substellar region, suppressing hurricane formation there.

Effect of bulk atmospheric composition

Atmospheric compositions on terrestrial exoplanets are unknown yet. Here we do a preliminary investigation of how atmospheric molecular weight influences hurricane formation under a uniform surface temperature of 301 K (see Methods). When the background atmosphere is set to H_2 or He, there is no hurricane, in contrast to the experiments of N_2, O_2, and CO_2 (Fig. 5), although GPI value is comparable to or even larger than that shown above. This is due to the fact that the condensate–H_2O is heavier than H_2 and He, so that any disturbance that brings water vapor upward will cause the density of a moist parcel to be larger than its surrounding environment, similar to the condition in Saturn's atmosphere (*36-38*). This process induces a negative buoyancy and stabilizes the atmosphere against convection. Simply, it can be understood using the ideal gas equation $p=\rho R_d T_v$ and the virtual temperature of

$$T_v = \frac{p}{p+(\epsilon-1)e} T, \quad (1)$$

where p is total air pressure, e is partial pressure of the condensate, ρ is air density, R_d is the gas constant of dry air, ϵ is the molecular weight ratio of water vapor to the dry air, and T is air temperature. For a H_2-dominated (or He-dominated) atmosphere, ϵ is equal to 9 (or 4.5), so that T_v is smaller than T. Therefore, a moist parcel is heavier than a dry parcel under the same p and T, and moist convection is inhibited, which is opposite to the condition on Earth. Moreover, in the experiments of N_2, O_2, and CO_2, a clear trend is that the hurricane size decreases as the mean molecular weight is increased. This is due to the fact that atmospheric scale height is inversely proportional to the mean molecular weight and subsequently the Rossby deformation radius (see Materials and Methods) becomes smaller.

Discussion

We find that hurricanes can form on tidally locked planets especially for those orbiting near the inner edge of the habitable zone of late M dwarfs. For planets in the middle range of the habitable zone, hurricanes are relatively fewer. Storm theories of Earth and Saturn can be used to understand the hurricane formation on tidally locked planets. Hurricanes can enhance the ocean mixing and oceanic heat transport from warmer to cooler regions in both horizontal and vertical directions. Hurricanes can also influence the transmission spectra of tidally locked planets. For instance, if hurricane moves to the terminator, water vapor concentration would increase largely (Fig. S7), which can influence the transmission signals. Unfortunately, present-day telescopes are not able to observe this (*39,40*) mainly due to the small-scale height of the atmosphere and the relatively small size of the hurricane to planetary radius. Differentiating them requires future large space telescopes or ground-based extremely large telescopes.

Materials and Methods

This section includes experimental design, hurricane detection method, and the calculations of genesis potential index and Rossby deformation radius.

Experimental Design. The model we used is the global Community Atmosphere Model version 4 (CAM4) with a dynamical core of finite volume (*41*). Deep convection is parameterized using the updated mass flux scheme of Zhang and McFarlane (*42*). Subgrid-scale momentum transport associated with convection is included (*43*). The parameterization of shallow moist convection is based on Hack (*44*). Condensation, evaporation, and precipitation parameterization is based on Zhang et al. (*45*) and Rasch and Kristjansson (*46*). Cloud fraction is diagnosed from atmospheric stratification, convective mass flux, and relative humidity. Realistic radiative transfer of water vapor, clouds, greenhouse gases, and aerosols are included.

The horizontal resolution we employed is 0.47o×0.63o in latitude and longitude, respectively. The number of vertical levels is 26. Planetary surface is covered by seawater everywhere (an aquaplanet). Because of the high resolution and the limited computational power, we specify surface temperature in the simulations. The surface temperature is set according to previous simulations of lower-resolution AGCMs coupled to a 50-m slab ocean (*47*,*48*). On the day side, the surface temperature is a function of latitude and longitude: $(T_{max} - T_{min})cos(\varphi)cos(\lambda) + T_{min}$ (shown in Fig. 2**A**), or $(T_{max} - T_{min})cos^{1/4}(\varphi)cos^{1/4}(\lambda) + T_{min}$ (shown in Fig. S3), where T_{max} is the maximum surface temperature, T_{min} is the minimum surface temperature, φ is the latitude, and λ is the longitude. On the night side, the surface temperature is uniform with a value of T_{min}. Three groups of T_{max} and T_{min} are used. One is for planets near the inner edge of the habitable zone, 315 K & 310 K. The other two are for planets in the middle range of the habitable zone, 308 K & 275 K and 301 K & 268 K; the power of 1/4 is used due to the very weak temperature gradients in the substellar region and strong temperature gradients near the terminators.

Planetary rotation period is set to be equal to orbital period, i.e., 1:1 spin-orbit resonance. Four rotation periods are examined: 6, 10, 20, and 40 earth days. For other types of spin-orbit resonance, such as 3:2 like Mercury, the climate is in the condition between the synchronous rotation and the very rapidly rotation of Earth (*49*), so that we have not done this kind of experiments. Planetary radius and gravity are set to be the same as Earth, but both obliquity and eccentricity are set to zero. Stellar temperature is set to 2600 or 3700 K; sensitivity test shows this has no significant effect on the results. The stellar radiation at the substellar point is set to 1300 or 1800 W m^{-2}; this also has no significant effect on the results because the surface temperature is fixed. By default, the mean surface pressure is 1 bar with ≈79% N_2 and ≈21% O_2. For greenhouse gases, we set CO_2 concentration to 367 parts per million by volume (ppmv), N_2O to 316 parts per billion by volume (ppbv), and CH_4 to 1760 ppbv. Ozone concentration is set to be the same as present-day Earth, which may influence the outflow temperature of hurricanes and the overshooting of extremely strong convection.

In order to briefly test the effect of atmospheric composition on the hurricane formation, we did several ideal experiments in which the background gas is set to H_2, He, N_2, O_2, and CO_2, respectively. The corresponding mean molecular weights are 2.02, 4.00, 28.01, 31.99, and 44.00 g $mole^{-1}$ and the corresponding specific heats (*50*) are 28.9, 20.8, 29.1, 29.5, and 37.2 J $mole^{-1}$ K^{-1}. We modify these two constants only. The model we employed (as well as most other global models) is unable to calculate the radiative transfer of dense H_2, He, O_2, or CO_2 and meanwhile surface temperatures under background gases differing from Earth have not been seriously examined. So, we choose to use globally uniform surface temperature (301 K) and stellar radiation (340 W m^{-2}) with neither seasonal nor diurnal cycle. Of course, this idealized thermal boundary condition is unrealistic, but it is able to avoid the effects of strong wind shear, baroclinic zone, cold surface, or other features that may inhibit hurricane formation or propagation (*51*). Two planetary rotation periods are used, one and three earth days.

Initial states of the experiments were from long-term (40 earth years) simulations using a lower resolution of $4^{o} \times 5^{o}$ or $1.9^{o} \times 2.5^{o}$ under the same experimental designs and parameterization schemes. Then, each experiment was run for five earth years under the high resolution, and the last four years were used to analyze below. As shown in Fig. 4, the southern hemisphere always has more hurricanes than the northern hemisphere; this may be due to some asymmetry in initial state or some stochastic process in the parameterizations.

Future work is required using AGCMs coupled to a slab ocean or using fully coupled atmosphere–ocean models. Moreover, future work is required to examine how continents influence the results. Hurricanes always decay quickly when they move over land because of the dramatic reduction in evaporation and the increase in surface roughness. Global climate models with more realistic cloud schemes and regional cloud resolving models with more accurate radiation transfer are required to simulate the hurricane genesis, especially for those who have quite different atmospheric compositions and/or air masses from Earth.

Hurricane detection. Hurricane formation and tracking is based on six hourly model output variables using the Geophysical Fluid Dynamics Laboratory tracking algorithm (*52*). Candidate hurricanes are identified by finding regions satisfying the following criteria: 1) the local 850-hPa relative vorticity maximum exceeds 3.5×10^{-5} s^{-1}; 2) the 850-hPa warm-core temperature must be at least 0.5 K warmer than the surrounding local mean; 3) the distance between the local sea level pressure minimum and the vorticity maximum should be within a distance of 2^{o} latitude or longitude, and so is the distance between the local sea level pressure minimum and the warm-core center; 4) the maximum 850-hPa wind speed exceeds ≈33 m s^{-1} at some time. These values of the thresholds influence the exact number of detected hurricanes but do not affect the main conclusions of this study.

Genesis Potential Index (GPI). The GPI is written as:

$$GPI = |10^5(\zeta + f)|^{3/2}(RH/50)^3\left(V_{pot}/70\right)^3(1.0 + 0.1 * V_{shear})^{-2}, \quad (1)$$

where ζ is the vertical component of relative vorticity, f is the planetary vorticity, RH is the relative humidity at the middle troposphere (600 hPa), V_{shear} is the wind shear of horizontal winds between the upper and lower troposphere (300 minus 850 hPa; or called vertical wind shear), and V_{pot} is potential intensity. V_{pot} is a measure of the maximum near-surface wind that can be maintained by hurricane under given environmental condition. Note that these parameters are not all independent; for instance, vertical wind shear can influence relative humidity.

The value of V_{pot} is calculated based on a local balance between thermal energy import and mechanical energy dissipation (*53,54*), written as

$$V_{pot} = \frac{C_k}{C_D}\frac{T_s - T_o}{T_o}[CAPE^* - CAPE^b]|_m, \quad (2)$$

where C_k is the exchange coefficient for enthalpy, C_D is the drag coefficient, T_s is the sea surface temperature, T_o is the mean outflow temperature, $CAPE^*$ is the convective available potential energy of air lifted from saturation at sea surface, and $CAPE^b$ is that of the boundary layer air. Both $CAPE^*$ and $CAPE^b$ are computed at the radius of maximum surface wind.

Rossby deformation radius. The Rossby radius of deformation (L_R) is the length scale at which rotational effects become as important as the effects of gravity waves or buoyancy in the evolution of the flow in a disturbance. L_R is equal to $\frac{NH}{f}$, where N is the Brunt-Vaisala frequency, and f is the Coriolis parameter. H is the scale height, equaling to $\frac{R^*\bar{T}}{M_d g}$, where R^* is the universal gas constant, $\bar{T}$ is the mean air temperature, M_d is the molar weight of the atmosphere, and g is the gravity (*55*). In idealized experiments with uniform surface temperature or uniform rotation, it is one of the rough scales that can be used for understanding hurricane size (*56-58*). In our experiments shown in Fig. 5, the value of L_R is ≈500-1500 km, comparable to the hurricane size. However, L_R

is strongly latitude-dependent because f is equal to $2\Omega sin(\varphi)$ (Ω is the rotation rate and φ is the latitude), but the hurricane size does not exhibit the same dependence. A better scaling was not found because of the nonlinear dynamics of hurricane and the complex interactions between hurricane and diabatic heating, environmental relative humidity, mesoscale convective system, and other features.

References

1. R. A. Anthes, *Tropical cyclones—their evolution, structure and effects.* (American Meteor Society, Boston, MA, 1982).
2. K. A. Emanuel, 100 Years of Progress in Tropical Cyclone Research. *Meteor. Monogr.* **59**, 15.1-15.68 (2019).
3. K. A. Emanuel, Contribution of tropical cyclones to meridional heat transport by the oceans. *J. Geophys. Res.* **106**, 14771-14781 (2001).
4. M. Jansen, R. Ferrari, Impact of the latitudinal distribution of tropical cyclones on ocean heat transport. *Geophys. Res. Lett.* **36**, 150-164 (2009).
5. H. Li, R. L. Sriver, Impact of Tropical Cyclones on the Global Ocean: Results from Multidecadal Global Ocean Simulations Isolating Tropical Cyclone Forcing. *J. Clim.* **31**, 8761-8784 (2018).
6. A. P. Showman, R. D. Wordsworth, T. M. Merlis, Y. Kaspi, *Atmospheric Circulation of Terrestrial Exoplanets.* (Univ Ariz Press, Tucson, AZ, 2013).
7. R. T. Pierrehumbert, M. Hammond, Atmospheric Circulation of Tide-Locked Exoplanets. *Annu. Rev. Fluid Mech.* **51**, 275-303 (2019).
8. R. K. Kopparapu et al. Habitable Moist Atmospheres on Terrestrial Planets near the Inner Edge of the Habitable Zone around M Dwarfs. *Astrophys. J.* **845**, 5 (2017).

9. J. Haqq-Misra, E. T. Wolf, M. Joshi, X. Zhang, R. K. Kopparapu, Demarcating circulation regimes of synchronously rotating terrestrial planets near the inner edge of the habitable zone. *Astrophys. J.* **852** (2017).
10. J. Yang, D. S. Abbot, D. B. Koll, Y. Hu, A. P. Showman, Ocean dynamics and the inner edge of the habitable zone for tidally locked terrestrial planets. *Astrophys. J.* **871**, 1-17 (2019).
11. A. D. Del Genio et al. Habitable climate scenarios for Proxima Centauri b with a dynamic ocean. *Astrobiology* **19**, 99-125 (2019).
12. M. Turbet et al. Modeling climate diversity, tidal dynamics and the fate of volatiles on TRAPPIST-1 planets. *Astron. Astrophys.* **612**, 1-22 (2018).
13. L. Carone, R. Keppens, L. Decin, Connecting the dots--II. Phase changes in the climate dynamics of tidally locked terrestrial exoplanets. *Mon. Not. R. Astron. Soc.* **453**, 2412-2437 (2015).
14. R. Wordsworth, Atmospheric heat redistribution and collapse on tidally locked rocky planets. *Astrophys. J.* **806**, 180 (2015).
15. A. L. Shields, S. Ballard, J. A. Johnson, The habitability of planets orbiting M-dwarf stars. *Phys. Rep.* **663**, 1-38 (2016).
16. M. M. Joshi, R. M. Haberle, R. T. Reynolds, Simulations of the Atmospheres of Synchronously Rotating Terrestrial Planets Orbiting M Dwarfs: Conditions for Atmospheric Collapse and the Implications for Habitability. *Icarus* **129**, 450-465 (1997).
17. T. M. Merlis, T. Schneider, Atmospheric dynamics of Earth-like tidally locked aqua-planets. *J. Adv. Model Earth Syst.* **2**, 13 (2010).
18. A. Edson, S. Lee, P. Bannon, J. F. Kasting, D. Pollard, Atmospheric circulations of terrestrial planets orbiting low-mass stars. *Icarus* **212**, 1-13 (2011).
19. R. T. Pierrehumbert, A palette of climates for Gliese 581g. *Astrophys. J. Lett.* **726**, L8-L12 (2011).

20. J. Leconte et al. 3D climate modeling of close-in land planets: circulation patterns, climate moist bistability and habitability. *Astron. Astrophys.* **554**, A19(2013).
21. K. Menou, Water-trapped worlds. *Astrophys. J.* **774**, 51 (2013).
22. S. Noda et al. The circulation pattern and day-night heat transport in the atmosphere of a synchronously rotating aquaplanet: dependence on planetary rotation rate. *Icarus* **282**, 1-18 (2017).
23. J. Checlair, K. Menou, D. S. Abbot, No snowball on habitable tidally locked planets. *Astrophys. J.* **845**, 132 (2017).
24. I. A. Boutle et al. Exploring the climate of Proxima B with the Met Office Unified Model. *Astron. Astrophys.* **601**, A120 (2017).
25. J. Bin, F. Tian, Y. Lin, Y. Wang, Low Probability of Tropical Cyclones on Ocean Planets in the Habitable Zones of M Dwarfs. *Icarus* **299**, 364-369 (2017).
26. J. G. Charney, A. Eliassen, On the growth of the hurricane depression. *J. Atmos. Sci.* **21**, 68-75 (1964).
27. R. K. Smith, On the theory of CISK. *Q. J. R. Meteorol. Soc.* **123**, 407-418 (1997).
28. Y. Q. Wang, Hurricane dynamics, in Tropical cyclones and hurricanes, *In: Zhang GRNP (ed) Encyclopedia of atmospheric sciences, 2nd edn.* (Academic Press, Oxford, 2015), pp. 8-29.
29. M. Yamasaki, A View on Tropical Cyclones as CISK. J. Meteorol. *Soc. Jpn.* **85B**, 145-164 (2007).
30. A. E. Gill, Some simple solutions for heat-induced tropical circulation. *Q. J. R. Meteorol. Soc.* **106**, 447-462 (1980).
31. A. P. Showman, L. M. Polvani, Equatorial superrotation on tidally locked exoplanets. *Astrophys. J.* **738**, 71 (2011).
32. T. Matsuno, Quasi-Geostrophic Motions in the Equatorial Area. *J. Meteorol. Soc. Jpn.* **44**, 25-42 (1966).

33. K. A. Emanuel, D. S. Nolan, Tropical cyclone activity and global climate. Preprints, *26th Conference on Hurricanes and Tropical Meteorology*, Miami, FL, Amer. Meteor. Soc. 240-241 (2004).

34. S. J. Camargo, K. A. Emanuel, A. H. Sobel, Use of a Genesis Potential Index to Diagnose ENSO Effects on Tropical Cyclone Genesis. *J. Clim.* **20**, 4819-4834 (2007).

35. B. Tang, K. A. Emanuel, Midlevel Ventilation's Constraint on Tropical Cyclone Intensity. *J. Atmos. Sci.* **67**, 1817-1830 (2010).

36. C. Li, A. P. Ingersoll, Moist convection in hydrogen atmospheres and the frequency of Saturn's giant storms. *Nat. Geosci.* **8**, 398-403 (2015).

37. J. Leconte, F. Selsis, F. Hersant, T. Guillot, Condensation-inhibited convection in hydrogen-rich atmospheres. *Astron. Astrophys.* **598**, A98 (2016).

38. T. Guillot, Condensation of methane, ammonia, and water and the inhibition of convection in giant planets. *Science* **269**, 1697-1699 (1995).

39. C. V. Morley, L. Kreidberg, Z. Rustamkulov, T. Robinson, J. J. Fortney, Observing the atmospheres of known temperate earth-sized planets with JWST. *Astrophys. J.* **850**, 121 (2017).

40. J. de Wit et al. Atmospheric reconnaissance of the habitable-zone Earth-sized planets orbiting TRAPPIST-1. *Nat. Astron.* **2**, 214-219 (2018).

41. R. Neale et al. *Description of the NCAR Community Atmosphere Model (CAM 4.0). NCAR Technical Note NCAR/TN-464+STR* (National Center for Atmospheric Research, Boulder, CO, 2010).

42. G. J. Zhang, N. A. McFarlane, Sensitivity of climate simulations to the parameterization of cumulus convection in the Canadian Climate Centre general circulation model. *Atmos.-Ocean* **33**, 407-446 (1995).

43. J. H. Richter, P. J. Rasch, Effects of Convective Momentum Transport on the Atmospheric Circulation in the Community Atmosphere Model, Version 3. *J. Clim.* **21**, 1487-1499 (2008).
44. J. J. Hack, Parameterization of moist convection in the National Center for Atmospheric Research community climate model (CCM2). *J. Geophys. Res.* **99**, 5551-5568 (1994).
45. M. Zhang, W. Lin, C. S. Bretherton, J. J. Hack, P. J. Rasch, A modified formulation of fractional stratiform condensation rate in the NCAR Community Atmospheric Model (CAM2). *J. Geophys. Res.* **108**, 4035 (2003).
46. P. J. Rasch, J. E. Kristjánsson, A Comparison of the CCM3 Model Climate Using Diagnosed and Predicted Condensate Parameterizations. *J. Clim.* **11**, 1587-1614 (1998).
47. J. Yang, N. B. Cowan, D. S. Abbot, Stabilizing cloud feedback dramatically expands the habitable zone of tidally locked planets. *Astrophys. J. Lett.* **771**, L45 (2013).
48. E. T. Wolf, R. K. Kopparapu, J. Haqq-Misra, Simulated Phase-dependent Spectra of Terrestrial Aquaplanets in M Dwarf Systems. *Astrophys. J.* **877**, 35 (2019).
49. J. Yang, G. Boue, D. C. Frabrycky, D. S. Abbot, Strong Dependence of the Inner Edge of the Habitable Zone on Planetary Rotation Rate. *Astrophys. J. Lett.* **787**, L2 (2014).
50. X. Zhang, A. P. Showman, Effects of Bulk Composition on the Atmospheric Dynamics on Close-in Exoplanets. *Astrophys. J.* **836**, 73 (2017).
51. T. M. Merlis, I. M. Held, Aquaplanet Simulations of Tropical Cyclones. *Curr. Clim. Change. Rep.* **5**, 185-195 (2019).
52. M. Zhao, I. M. Held, S. J. Lin, G. A. Vecchi, Simulations of Global Hurricane Climatology, Interannual Variability, and Response to Global Warming Using a 50-km Resolution GCM. *J. Clim.* **22**, 6653-6678 (2009).
53. K. A. Emanuel, The maximum intensity of hurricanes. *J. Atmos. Sci.* **45**, 1143-1155 (1988).
54. M. Bister, K. A. Emanuel, Low frequency variability of tropical cyclone potential intensity 1. Interannual to interdecadal variability. *J. Geophys.Res.* **107,** ACL 26-21-ACL 26-15 (2002).

55. J. M. Wallace, P. V. Hobbs, *Atmospheric Science: An Introductory Survey. 2nd ed.* (Academic Press, 2006).
56. I. M. Held, M. Zhao, Horizontally homogeneous rotating radiative-convective equilibria at GCM resolution. *J. Atmos. Sci.* **65**, 2003-2013 (2008).
57. D. R. Chavas, N. Lin, W. Dong, Y. Lin, Observed tropical cyclone size revisited. *J. Clim.* **29**, 2923-2939 (2016).
58. D. R. Chavas, K. A. Reed, Dynamical Aquaplanet Experiments with Uniform Thermal Forcing: System Dynamics and Implications for Tropical Cyclone Genesis and Size. *J. Atmos. Sci.* **76**, 2257-2274 (2019).

Acknowledgments: We thank the National Center for Atmospheric Research (NCAR) groups for developing the model CAM4 and making it available to public. We are grateful to the discussions with Hao Fu, Gan Zhang, Cheng Li, Weixin Xu, Yongyun Hu, and Zhiyong Meng. **Funding:** J.Y. is supported by the Chinese National Science Foundation under grants 41675071 and 41861124002.
Author contributions: J.Y. led the project, performed the numerical experiments, and wrote the manuscript. M.Y. did the data analyses and plotted the figures. Both J.Y. and M.Y. contributed to improve the manuscript. **Competing interests:** There is no any competing interests. **Data and materials availability:** The data that support the plots within this paper will be stored on a public structured data repository after the paper accepted. The source codes of the model can be downloaded from http://www.cesm.ucar.edu/models/, and changes of the model are available from the authors J.Y. junyang@pku.edu.cn and M.Y. yanmy@pku.edu.cn.

Figures 1-5:

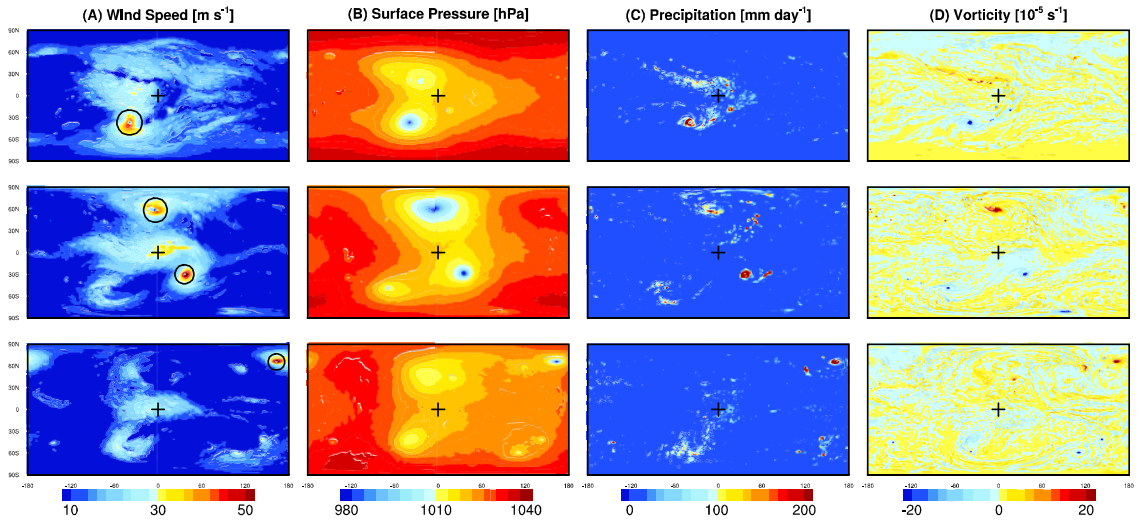

Fig. 1. Snapshots of hurricanes on a tidally locked aqua-planet near the inner edge of the habitable zone in the control experiment. From left to right, the variables are instantaneous wind speed at 850 hPa, surface air pressure, precipitation, and the vertical component of relative vorticity at 850 hPa, respectively. From upper to bottom, they are for three different moments. The four hurricanes are marked with black circles over the wind speed panels. The black cross is the substellar point in this figure and hereafter. See Video S1 online for the evolution of the hurricanes.

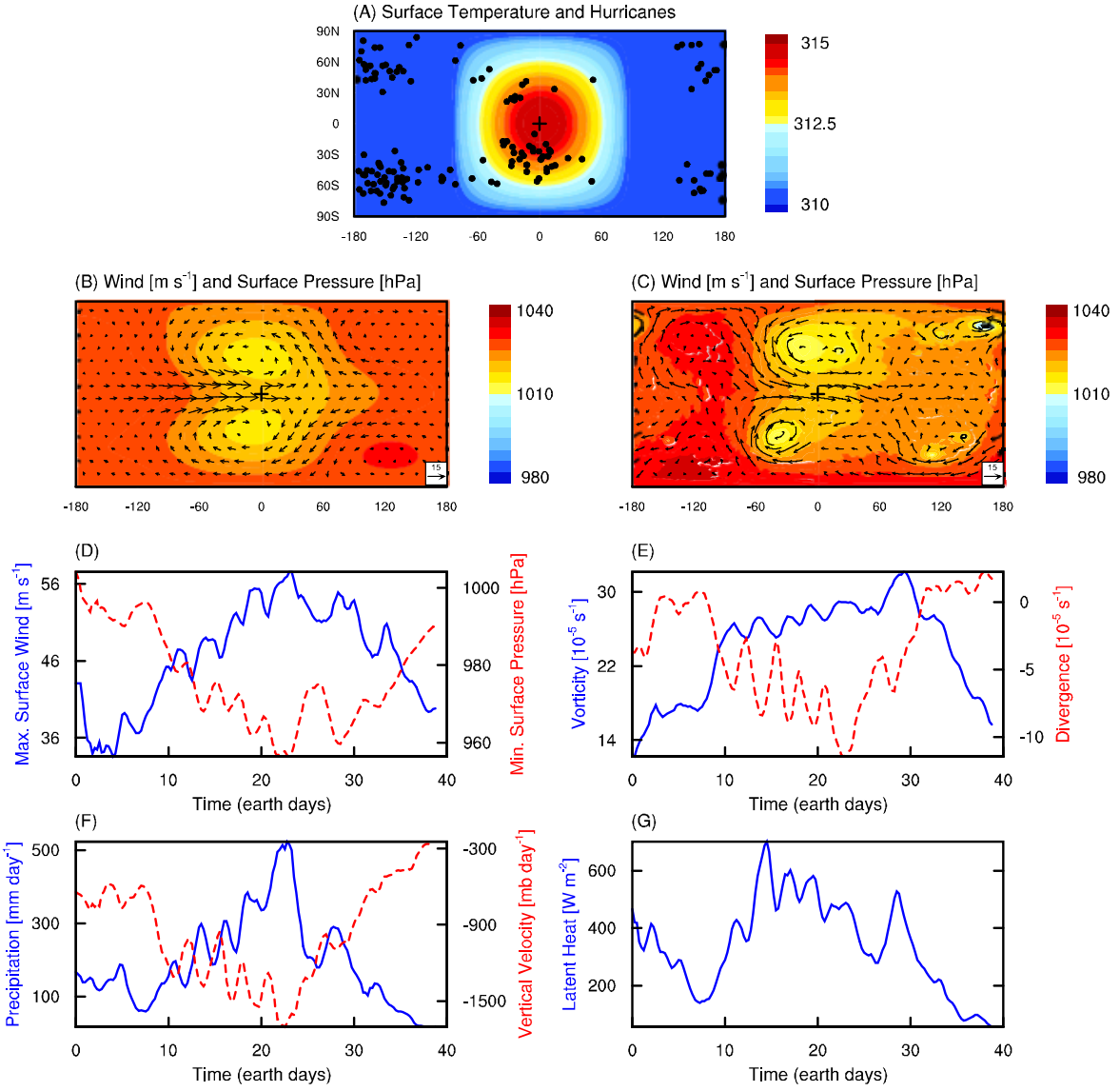

462

463 **Fig. 2. Mechanisms for hurricane formation in the control experiment.** (**A**): The location of
464 hurricane formation (dots) and surface air temperature (color shading). The number of hurricanes
465 during the four-years integration is 154. (**B**): Long-term mean surface air pressure (shading) and
466 winds at 850 hPa (vector). (**C**): Same as (**D**) but for an instantaneous. The life cycle of one hurricane
467 on the day side: (**D**): maximum surface wind speed (blue) and minimum surface pressure (red), (**E**):
468 relative vorticity (blue) and divergence (red) at 850 hPa, (**F**): precipitation (blue) and vertical
469 velocity at 850 hPa (red), and (**G**): surface latent heat flux (blue). For (**E**), (**F**) and (**G**), the variables
470 are calculated for area mean of 500×500 km2 around the low-pressure center.

471

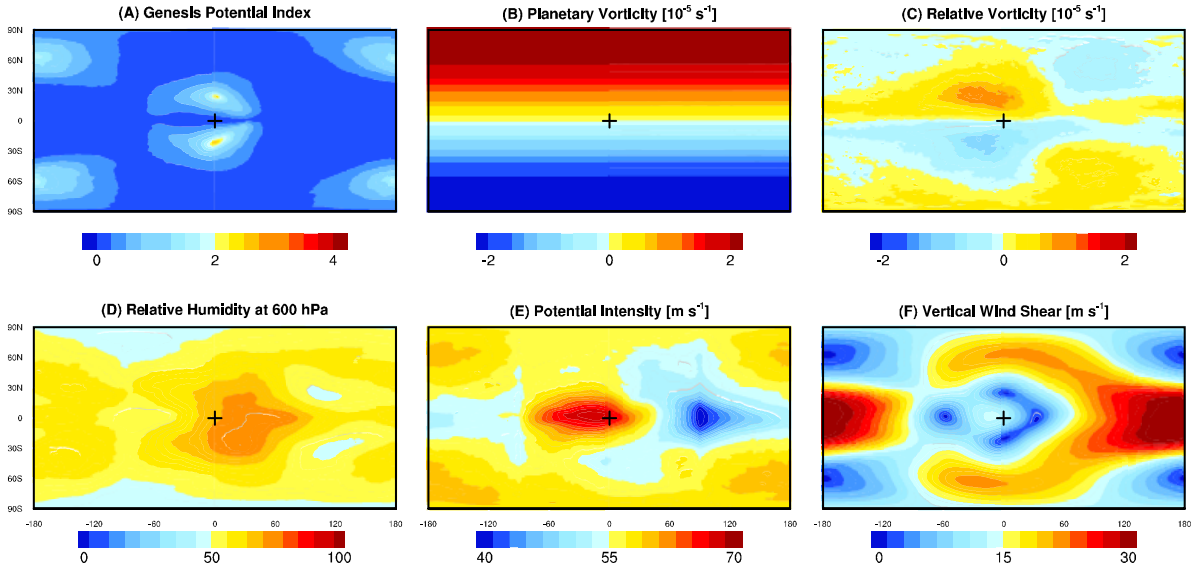

Fig. 3. Environmental condition for hurricane formation. (**A**): Genesis potential index (GPI); (**B**): planetary vorticity; (**C**): long-term mean relative vorticity at 850 hPa; (**D**): relative humidity at 600 hPa; (**E**): potential intensity; (**F**): vertical shear of the horizontal winds between 300 and 850 hPa. Note the environmental vorticity in panel (**C**) is one order smaller than the vorticity of hurricanes shown in Fig. 1**D**.

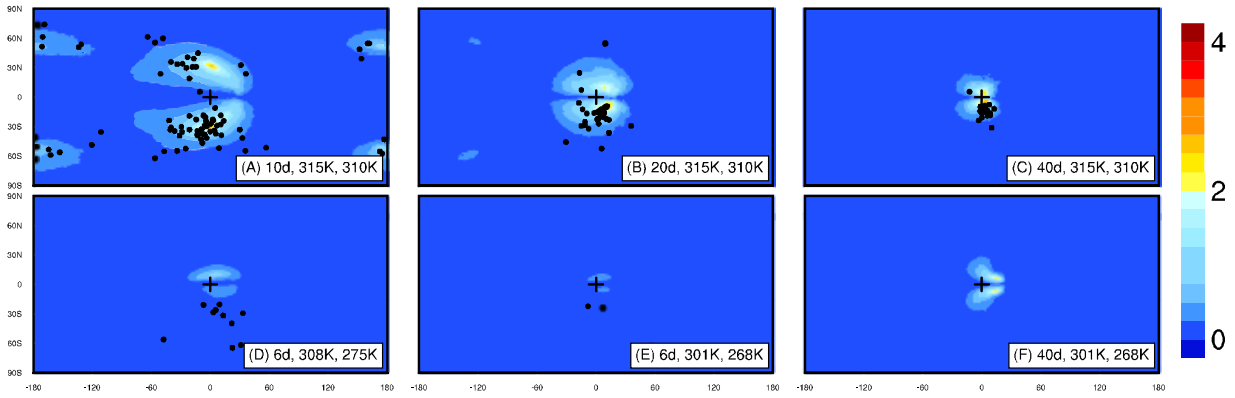

Fig. 4. Effects of planetary rotation and surface temperature on hurricane formation (dots) and the GPI (color shading). Experiments are for varying rotation period (**A**-**C**), varying surface temperature (**D**-**E**), and varying both (**F**). Experimental designs are the same as the control experiment in Fig. 1 except that the rotation period is set to (**A**): 10, (**B**): 20, and (**C**): 40 earth days; (**D**): the maximum surface temperature is reduced from 315 to 308 K and the night-side surface temperature is reduced from 310 to 275 K (see Fig. S3**A**); (**E**): same as (**D**) but for 301 K and 268 K, respectively (see Fig. S3**B**); and (**F**) same as (**E**) but for a rotation period of 40 earth days. The number of hurricanes is 88, 34, 21, 10, 2, and 0, respectively. See Fig. S4 for the snapshots of typical hurricanes.

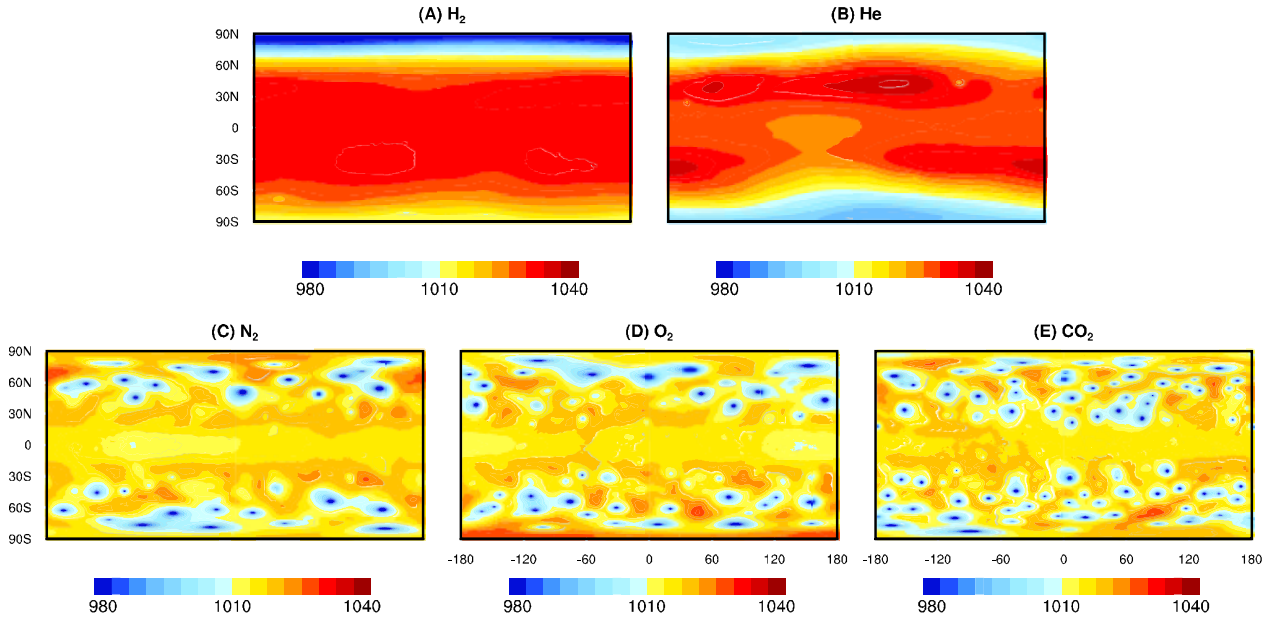

510

511 **Fig. 5. Effects of background gases on hurricane formation.** From (**A**) to (**E**), they are snapshots
512 of instantaneous surface air pressure (hPa) under background gases of H_2, He, N_2, O_2, and CO_2,
513 respectively. In all these experiments, the planetary rotation period is 1 earth day and surface
514 temperature is uniform (301 K). For experiments with a rotation period of 3 earth days, the results
515 are the same except that the hurricanes are larger in size but less in number in the latter three
516 experiments.